Planning Smooth and Obstacle-Avoiding B-Spline Paths for Autonomous Mining Vehicles

Tomas Berglund, Andrej Brodnik, *Member, IEEE*, Håkan Jonsson, Mats Staffanson, and Inge Söderkvist

***Abstract*—We study the problem of automatic generation of smooth and obstacle-avoiding planar paths for efficient guidance of autonomous mining vehicles. Fast traversal of a path is of special interest. We consider four-wheel four-gear articulated vehicles and assume that we have an *a priori* knowledge of the mine wall environment in the form of polygonal chains. Computing quartic uniform B-spline curves, minimizing curvature variation, staying at least at a proposed safety margin distance from the mine walls, we plan high speed paths.**

We present a study where our implementations are successfully applied on eight path-planning cases arising from real-world mining data provided by the Swedish mining company Luossavaara–Kiirunavaara AB (LKAB). The results from the study indicate that our proposed methods for computing obstacle-avoiding minimum curvature variation B-splines yield paths that are substantially better than the ones used by LKAB today. Our simulations show that, with an average 32.13%, the new paths are faster to travel along than the paths currently in use. Preliminary results from the production at LKAB show an overall 5%–10% decrease in the total time for an entire mining cycle. Such a cycle includes both traveling, ore loading, and unloading.

***Note to Practitioners*—This article was motivated by the problem of how to automatically produce high quality drive-paths for autonomous transportation vehicles in mines. The vehicles are heavy ($>$ 100 tonnes) but are still expected to run at speeds up to 20 km/h to be productive. To reach these speeds without damaging the steering gear and the mechanics of the vehicles, their paths need to be smooth. It turns out that visual inspection is often insufficient to produce a path with high smoothness. We suggest a method for computing paths, requiring an *a priori* knowledge about the environment, that minimizes the amount of steering needed. The computed paths are safe as they guarantee no collisions between the vehicle and the tunnel wall. We present a study of eight cases based on real-world application data from the Swedish mining company Luossavaara-Kiirunavaara AB (LKAB) showing that, with an average of 32.13%, our paths are faster to travel along than the paths currently in use.**

***Index Terms*—Articulated vehicle, autonomous guided vehicle (AGV), B-spline curve, derivative of curvature, mining industry, motion-planning, nonlinear optimization, obstacle-avoidance, path-planning, safety margin, smoothness, travel time.**

I. Introduction

Path-planning is a problem area growing more and more important as the level of automation increases [1]–[7]. Today, there are many industrial applications that require the pre-computation of paths for autonomous vehicles and robot arms [8]–[13]. We address the problem of computing an obstacle-avoiding planar path that combines the properties of being both smooth and fast to traverse.

1) Obstacles: The work space of autonomous vehicles and robot arms are often cluttered with obstacles that must be avoided. We work with the path-planning of the autonomous vehicles used for transporting iron ore in the underground mines of the Swedish mining company Luossavaara-Kiirunavaara Aktiebolag (LKAB) [14] . It is crucial that these autonomous vehicles avoid the obstacles constituted by the mine walls in order for the production to proceed. Much work has been devoted to planning paths in the presence of obstacles. Many results involve piecewise linear paths [3], [15].

2) Smoothness: Practical applications involving physical machines require that paths are smooth [5], [7], [16]–[18]. The autonomous ore transport vehicle used at LKAB is articulated. This means that the whole vehicle is involved in the steering. Its steering gear gets worn out by jerks in its path. Large jerks increase the risk of slippage and dropping of ore. This might even lead to halting production.

Depending on context, a path or curve in space is said to be smooth if it is tangent continuous, has a continuous curvature, or even has a continuous derivative of curvature [5], [7], [16]–[18]. We work with quartic B-spline functions. These have a continuous derivative of curvature.

3) Speed: Here, an important aspect of the smoothness of a path is its relation to the speed at which the path can be traversed. With or without gears, the turning speed of a vehicle is limited by the speed of the vehicle. The gear and the speed need to be adjusted for admitting the vehicle to follow the path. If there is a high smoothness of the path, high gears can be used for a longer time, giving a fast traversal of the path.

4) Safety: Still, obstacle-avoidance and smoothness are not enough for practical purposes. The path should also stay at a sufficient distance—the safety margin—from the obstacles. A path will tend to go close to obstacles in order to have an as high smoothness as possible. This means that the path will most likely touch the safety margin. The computation of safety margins has been considered in the literature [19]. We propose a method for computing safety margins that can be utilized in our addressed environment of mine walls.

5) Contribution: We put to test the assumption that geometrically smooth paths, computed with an *a priori* knowledge about the environment, are fast to traverse. The Swedish mining company LKAB provides us with a set of piecewise seventh-degree polynomial that they have already planned.

Based on mine map application data from LKAB, in the form of polygonal chains, we compute safety margins described by two flanking polygonal chains. Inside of these margins, using the fact that we work with polygonal chains, we can use a standard nonlinear programming tool to compute geometrically smooth paths built from obstacle-avoiding quartic minimum curvature variation B-spline curves. These quartic B-splines have a continuous derivative of curvature.

Using the same model of a four-gear four-wheel articulated vehicle with prescribed gear-limits as the one used by LKAB, we observe that it is possible to travel at a higher speed along the B-spline paths than along the corresponding LKAB paths. This is presented by considering eight scenarios.

II. Preliminaries

This section contains a description of the LKAB paths and their representation, our smoothness measure, and a motivation for using B-splines as a path representation. It also contains a description of our minimum curvature variation B-spline (MVB) and how it is computed.

Manuscript received June 03, 2008; revised November 10, 2008. First published May 27, 2009; current version published January 08, 2010. This paper was recommended for publication by Associate Editor Y. S. Wong and Editor M. Wang upon evaluation of the reviewers' comments. This work was supported in part by the Swedish mining company LKAB and the Research Council of Norrbotten (Norrbottens Forskningsråd) under Contract NoFo 04-005.

T. Berglund, H. Jonsson, and M. Staffanson are with the Luleå University of Technology, Department of Computer Science and Electrical Engineering, Sweden SE-971 87 (e-mail: tomas.berglund@ltu.se; hakan.jonsson@ltu.se ; mats.staffanson@ltu.se).

A. Brodnik is with the University of Primorska, PINT, Slovenia, SI-6000 and with the University of Ljubljana, Faculty of Computer and Information Science, Slovenia SI-1000 (e-mail: andrej.brodnik@upr.si).

I. Söderkvist is with the Luleå University of Technology, Department of Mathematics, Sweden SE-971 87 (e-mail: inge.soderkvist@ltu.se).

Color versions of one or more of the figures in this paper are available online at http://ieeexplore.ieee.org.

Digital Object Identifier 10.1109/TASE.2009.2015886

As a brief explanation of our algorithm, we also present a brief method overview.

1) Path Cycles and Segments: Our interest lies in the properties and planning of a path going from an initial to a terminal posture or pose. In industry, such a path is commonly denoted as a path cycle. We also use the term path cycle. A path is built from subpaths, i.e., consecutive path segments.

2) MVB Paths and Constraints: We compute paths that are quartic minimum curvature variation B-spline (MVB) curves (see Section II). All paths meet up with initial and terminal endpoint constraints, which are given in terms of position, slope angle, curvature, and derivative of curvature. Furthermore, the paths must not intersect obstacles represented by two flanking polygonal chains generated from mine wall information. The linear functions that describes our obstacles comes from connected laser point data measurements at LKAB.

3) LKAB Paths: LKAB describes path segments by seventh-degree polynomials parameterized in separate coordinate systems. For each polynomial segment, the maximal derivative of curvature is minimized. These paths are flexible but they do not necessarily minimize curvature variation or smoothness over the whole path. This means that the traversal time for the entire path need not be optimized.

4) Smoothness Measure: We consider a smoothness measure described by e.g., Kanayama and Hartman [20]. This measure is the integral over the square of arc-length derivative of curvature along the path. A motivation of using this measure comes from the physics of motion. The variation of curvature is proportional to the jerk or change in lateral acceleration of the vehicle. Jerks are unwanted for a vehicle for many reasons. They also negatively affect the speed of the vehicle.

We consider curves being functions along a room axis. A function $f(x)$ with curvature $K(x)$, $x \in [x_0, x_1]$, can be parameterized in its arc length s. With standard room transformations in the plane, using the notation $\dot{\nu} = d\nu/ds$ and $\nu' = d\nu/dx$, we express our cost function as

$$\int_{s(x_0)}^{s(x_1)} \dot{K}(s)^2 \, ds = \int_{x_0}^{x_1} \frac{K'(x)^2}{\sqrt{1 + f'(x)^2}} \, dx. \tag{1}$$

5) Different Curve Types: There are many ways to represent curves used for trajectory planning. Seven different curve types are mentioned in an overview [6]. Line segments coupled with arcs of circles, Cartesian polynomials, clothoids coupled with anticlothoids, cubic spirals, generalized polar polynomials, B-splines, and parametric curves being sums of harmonics (sine and cosine functions). Each of the four first mentioned curve types have their drawbacks.

Curves built from line segments and arcs of circles have discontinuities in their curvature leading to unwanted jerks. And the maximum value of curvature of Cartesian polynomials is not easily computed. Clothoids and anticlothoids are intrinsic curves meaning that there are no closed form expressions for their position [5], [7]. Cubic spirals have the same disadvantage. The three remaining curve types do not have the same drawbacks. They can all be written in closed form and they allow any number of continuous derivatives.

6) B-Spline Curves: We work with curves built from B-spline functions. B-spline functions [21]–[23] have properties making them suitable for smooth and obstacle-avoiding path-planning. They are efficiently computed closed form functions [21]. Their approximation ability and the properties of their shape depend on the number of B-spline basis functions used for defining them [24]. They are widely used in data fitting, computer aided design (CAD), automated manufacturing (CAM), and computer graphics [25].

A B-spline function or B-spline $B(x)$ is a piecewise polynomial of a certain degree. Much work has been devoted to planning or smoothing trajectories using B-splines [8]–[13]. However, this work does not handle obstacle-avoidance and it involves B-splines having a discontinuous curvature. We consider quartic, i.e., degree 4, uniform B-splines $B(x)$. A quartic B-splines has an inherited continuous derivative of curvature which leads to small jerks.

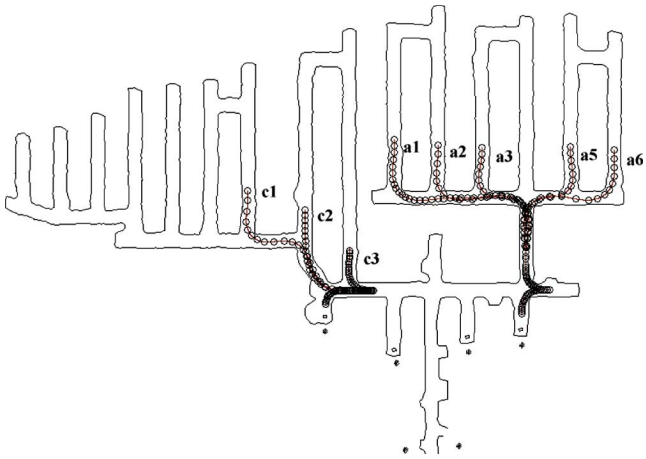

Fig. 1. Mining area 820:39 in the LKAB underground mine in Kiruna, Sweden. The ore is produced using autonomous vehicles. We study the eight path cycles a1, a2, a3, a5, a6, c1, c2, and c3. With increasing smoothness of a cycle comes an increase in speed and a shortening of travel time.

7) B-Spline Envelope: It is possible to compute an envelope containing the B-spline function [26], [27]. By means of the envelope, the B-spline function can avoid obstacles represented by piecewise linear functions $\underline{c}(x) \leq \bar{c}(x)$. The envelope of $B(x)$ is itself a pair of piecewise linear functions $\underline{e}(x)$ and $\bar{e}(x)$, given by $B(x)$, such that $\underline{e}(x) \leq B(x) \leq \bar{e}(x)$. For obstacles-avoidance it suffices to impose the constraints $\underline{c}(x) \leq \underline{e}(x)$ and $\bar{e}(x) \leq \bar{c}(x)$. An optimization problem with a finite number of linear constraints can then be formulated.

8) Minimum Curvature Variation B-Spline (MVB): We are concerned with obstacle-avoiding minimum curvature variation B-splines (MVB) [28], [29]. They are solutions to:

9) Problem 1: Given two flanking obstacles in the form of polygonal chains that are piecewise linear functions $\underline{c}(x) \leq \bar{c}(x)$ defined on a real interval $I = [x_0, x_1]$, a set of endpoint constraints, and n B-spline basis functions, compute a quartic uniform B-spline $B(x)$ defined on I such that

1) the B-spline $B(x)$ satisfies the given endpoint constraints,
2) $\underline{c}(x) \leq \underline{e}(x)$ and $\bar{e}(x) \leq \bar{c}(x)$, and
3) the B-spline $B(x)$ minimizes the cost function

$$\int_I \frac{K'(x)^2}{\sqrt{1 + B'(x)^2}} dx \tag{2}$$

where $K(x) = B''(x)/(1 + B'(x)^2)^{3/2}$ is the curvature and $\underline{e}(x) \leq \bar{e}(x)$ is the envelope of $B(x)$ respectively.

This linearly constrained nonlinear optimization problem can be solved with standard optimization tools. One such tool is the MATLAB solver `fmincon` which in this case uses a medium scale optimization algorithm based on Sequential Quadratic Programming (SQL) [30]. A uniform knot placement is considered in this paper. We use the integration routine `coteglob` [31]. In comparison with other routines, we find it to have an overall high accuracy. Fig. 5 shows a computed MVB. It is seen how the envelope contains the B-spline curve and restricts it from touching the obstacles.

It is sometimes insufficient to work with one room axis only. In certain situations, the problem of finding an MVB path is divided into into subproblems. Introducing additional room axes is today a manually solved problem.

Fig. 2. Side view of the Tamrock Toro 2500 electrical wheel loader; length: 14 meters, operating weight: 76 tonnes, and capacity: 25 tonnes.

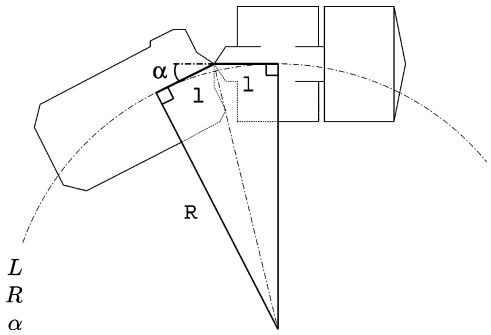

Fig. 3. Model of the Tamrock 2500 electrical wheel loader seen from above. The right part represents the front of the vehicle. The model is used for maneuverability computations that in turn are used for computing the gear shifting scheme for a path traversal. The vehicle has four distinct gears.

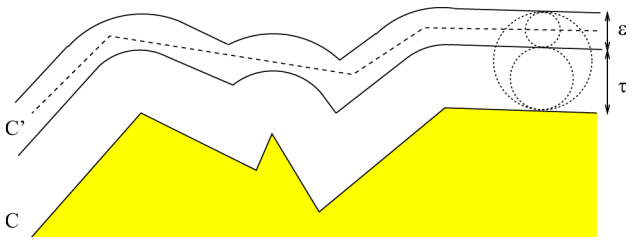

Fig. 4. To keep the vehicle at a safe distance from the walls of the mine, a safety margin is computed from laser data describing the mine walls as polygonal chains. Here is seen one side of the mine tunnel from above. The polygonal chain C' approximates C. The minimal distance between a point on C' and a point on C lies between τ and $\tau + \epsilon$. The approximation is made to decrease the number of vertices as this decreases the amount of input for the optimization problem. To leave space for the computation of a B-spline function, we assume that $2(\tau + \epsilon)$ is smaller than the width of the corridor.

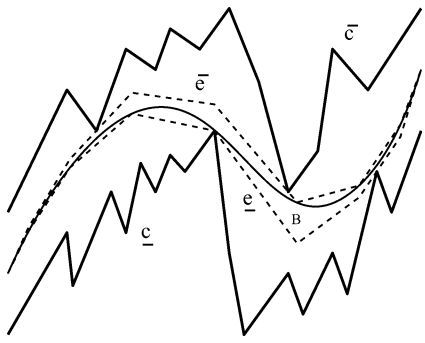

Fig. 5. Computed minimum curvature variation B-spline (MVB), B, contained in its envelope $\underline{e} \leq \bar{e}$ which in turn is situated between two obstacles described by polygonal chains $\underline{c} \leq \bar{c}$. It is seen that the envelope stops the B-spline from touching the obstacles as $\underline{c} \leq \underline{e} \leq B \leq \bar{e} \leq \bar{c}$. With the envelope, our optimization problem for finding the curve with the highest smoothness gets a finite number of constraints. These even become linear.

10) Method Overview: For different path cycles, we want to compare the properties of our MVB paths with the properties of the corresponding paths generated at LKAB. We are given the corridor-like environment, the LKAB paths with their gear shifting scheme, the cost function, the vehicle model, and the start and endpoint constraints. For each comparison we do the following.

1) Compute safety margins giving a new and narrower corridor environment.
2) Plan an obstacle-avoiding MVB path by solving a linearly constrained optimization problem.
3) Compute the highest possible gear for the vehicle on each MVB path segment.
4) Compare the MVB path cycle with the corresponding LKAB path cycle when it comes to traversal time, value of the cost function, maximum curvature, maximum derivative of curvature as well as path length.

TABLE I
TAMROCK 2500 GEAR SPEEDS AND ACCELERATIONS

Gear	Measured speed (m/s)	Acceleration (m/s^2)
1	1.0	3.8
2	1.9	1.3
3	3.1	0.8
4	5.0	0.5

III. VEHICLE MODEL AND SAFETY MARGIN

We use a vehicle model based on the Load-Haulage-Dump vehicle Tamrock Toro 2500 used at LKAB [32]. It is an electrical wheel loader with articulated steering, seen in Fig. 2. In our case it is fully automated. We model the sweep area of the vehicle during its movement as being of circular shape. This is used to compute the safety margin.

1) Gears, Speed and Acceleration: The vehicle has an electrical engine and four distinct or discrete gears. On average, the wheel power output is about 165kW. Based on measurements made at LKAB, the vehicle mean weight is set to 85 tonnes.

LKAB has measured the average driving speed of each gear and the average acceleration up to each gear. These values are presented in Table I. All gears have the deceleration of 0.9 meters per second square. On every segment, the highest gear possible is chosen. The reason for not having the very highest gear all the time is the limits in maneuvrebility.

2) Travel Time: The total path cycle travel time is the sum of the time to travel along each of its segments. The speed over a segment may contain acceleration, a constant speed stretch and deceleration. In tests, the constant speed is reached on every segment. In our model also, we allow the vehicle to reach constant speed on each segment.

To compute the travel time, we model the vehicle movement along a path segment. Let a be the acceleration, d the deceleration, and v_c the constant speed. Furthermore, let v_i, v_t, and l be the initial speed, terminal speed, and the length of the segment, respectively. As shown in Fig. 6, the time $t_a = (v_c - v_i)/a$ of acceleration and the time $t_d = (v_c - v_t)/d$ of deceleration can be used to compute the arc-lengths s_a, s_d, and s_c of acceleration, deceleration, and constant speed, respectively, through $s_a = at_a^2/2 + v_i t_a$, $s_d = dt_d^2/2 + v_t t_d$, and $s_c = l - s_a - s_d$. Then, the total time t_{tot} is found to be

$$t_{tot} = t_a + \frac{s_c}{v_c} + t_d = \frac{(v_c - v_i)^2}{2av_c} + \frac{l}{v_c} + \frac{(v_c - v_t)^2}{2dv_c}. \quad (3)$$

3) Limits in Maneuverability: The LKAB vehicle has a limited maneuverability. When designing paths, the steering angle α of the vehicle is limited to $|\alpha| \leq \alpha_{\max} = 38^\circ$ and the time derivative $d\alpha/dt$ of the steering angle is limited to $|d\alpha/dt| \leq \dot{\alpha}_{\max} = 10^\circ$ per second.

A model of the vehicle is built from its technical specification. Fig. 3 shows a drawing of the vehicle. The distance $L = 2.55$ meters to the

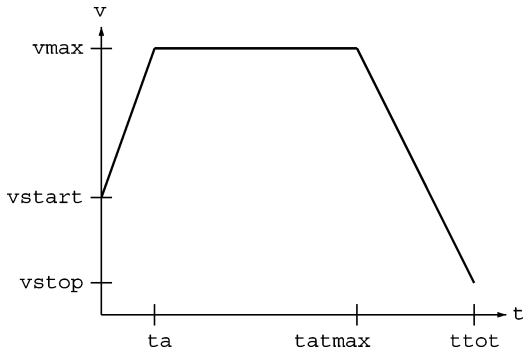

Fig. 6. An entire path cycle is a concatenation of a number of path segments. Every segment has a prescribed gear. The gear is chosen to be the highest possible. That is after maneuverability limitations are accounted for. This figure contains a graph, used in our speed model, showing how the speed of the vehicle can be changed over a path segment. This allows for time calculations for the entire path.

joint is the same for both the front and the rear wheels. The radius of curvature is denoted R. The curvature K is calculated according to $K = 1/R = \tan(\alpha/2)/L$.

We let v and s be the vehicle speed and curve length parameter respectively. After some calculations involving the constraint given by $\alpha_{\max}$, it is possible to isolate $d\alpha/dt$ and establish the bound

$$\left| \frac{v}{(1 + L^2K^2)} \frac{dK}{ds} \right| \leq \frac{\dot{\alpha}_{\max}}{2L}. \tag{4}$$

For each path segment, the gear with the highest prescribed velocity is chosen such that this bound still holds.

4) Safety Margin: To account for the sweep area of the vehicle and at the same time impose a safety distance between the vehicle and the mine walls, we compute a safety margin.

We use the Minkowski sum [19] on a polygonal chain to account for the size of a vehicle. As the result is a polygonal chain for use in our optimization problem, we are interested in keeping the number of vertices as low as possible. The safety margin problem can be formulated as:

5) Problem 2: Given a polygonal chain C construct another polygonal chain C', containing no point closer to C than τ and no point farther from C than $\tau + \epsilon$, having as few vertices as possible.

A plot of an instance of the problem is shown in Fig. 4. A solution to this problem is presented by Iri and Imai [33]. We solve a restricted version of the problem where the resulting polygonal chain has its vertices at distance $\tau + \epsilon/2$ from C.

IV. Path Cycle Comparisons

From two polygonal chains we can compute a safety margin. The B-spline envelope allows the computation of an obstacle-avoiding MVB path satisfying start and endpoint constraints. These methods are presented in previous work [28].

Here, we compare our paths with corresponding real-life paths produced in industry. In this case we apply our methods on data from LKAB. To a great extent, these industrial paths are manually generated. We use the same vehicle and time model as the one used at LKAB, see Section III. Properties of our computed MVB paths are compared with those of the corresponding LKAB paths. Especially, we put an interest in comparing travel times along a path cycle. The comparison is made without taking into account any control algorithms.

The LKAB paths are built from consecutive seventh degree polynomial path segments. They are not generated to minimize curvature variation. Our MVB path is a fourth-degree B-spline function defined along a room axis. It minimizes curvature variation and is divided into segments according to Section III. For certain geometries, where more than one room axis is needed or preferable, the problem of computing an MVB path is split into subproblems.

1) LKAB Mining Area 820:39: We consider mining area 820:39 in the LKAB underground mine in Kiruna, Sweden. This mining area is shown in Fig. 1. The figure points out eight path cycles, namely a1, a2, a3, a5, a6, c1, c2, and c3. A safety margin is computed such that it accounts for both the sweep area of the vehicle and takes into consideration the safety distance used at LKAB. In our setting, the safety margin lies in a region between 2.25 m and 2.35 m from the polygonal chains describing the walls of the mine ($\tau = 2.25$ m and $\epsilon = 0.10$ m in the safety margin problem of Section III).

The MVB paths are computed to satisfy the same endpoint constraints as those of the LKAB paths. Derivative of curvature and curvature are numerically computed at 300 positions along each path segment. For both the MVB and the LKAB paths, according to the same rules, the highest possible gear is chosen on each segment, see Section III. Also, according to Section III, the acceleration and deceleration along an MVB path and an LKAB path are computed in the same way. An average weight of 85 tonnes is used in our computations. This is a weight also proposed by LKAB.

To suit the settings studied here, we compute an entire MVB path cycle by dividing it into connected subpaths. Each subpath is a 25 basis B-spline function defining a set of path segments. When an LKAB is generated, each and every segment is defined manually. The splitting is only performed when more than one room axis is preferable. We follow a scheme where a split-point is introduced where the corridor has a slope change of more than about 40 degrees and, where possible, in the middle of a straight stretch of the road.

2) Path Cycle a1: We give a detailed presentation of one of the eight path cycle comparisons. This is for cycle a1, seen in Fig. 7(a). The cycle starts at the initial position I in the upper left corner and ends at the terminal position T at the bottom right. The detour just above T is due to the position of the vehicle power cable outlet.

The difference between the MVB and the LKAB gear shifting and velocities is shown in Fig. 7(b). Positive numbers means that the vehicle is driving forwards and vice versa. The MVB path cycle is slightly longer than the LKAB path (184.7 m vs 183.2 m as seen in Table II), but being traversed, it allows higher speed most of the time being traversed.

Fig. 8 shows a comparison between the derivatives of curvature of the MVB and the LKAB paths along cycle a1. The values along the MVB path have an overall lower magnitude those along the LKAB path.

For the remaining seven path cycles, we get similar results as those for cycle a1. Results from all eight comparisons are presented in Table II. Letting m stand for meters, rad for radians and s for seconds, the columns of the table show the following properties of an entire curve:

t	total path traversal time (s);
S_{cost}	smoothness cost $\int \dot{K}(s)^2 ds (rad^2/m^3)$;.
$K_{\max}$	max magnitude of curvature (rad/m);
$\dot{K}_{\max}$	max magnitude of derivative of curvature (rad/m^2);
s	total path length (m).

The rows of Table II are divided into groups depending on what cycle they belong to. Each cycle has a row for LKAB, MVB, and a difference in percents going from the LKAB value to the MVB value. The last row of the table presents an average of all the percentage differences.

Even though being slightly longer, it is seen that the MVB path is both smoother and faster to traverse than the LKAB path. An optimization with 25 basis functions takes about 30 minutes on a Pentium IV 2 GHz machine with 2 Gb RAM memory.

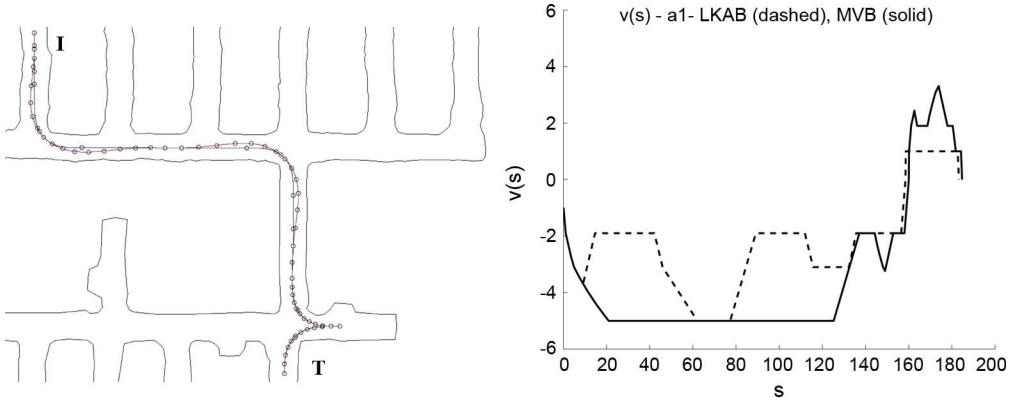

(a) (b)

Fig. 7. Cycle a1: LKAB (dotted/slashed) and MVB (solid). Two subfigures showing both the LKAB and the MVB curves in the mining environment as well as the velocity over curve length along the two curves. The MVB curve is slightly longer than the LKAB curve, see Table II. (a) Cycle a1: LKAB (dotted) and MVB (solid). This subfigure shows the LKAB path together with the computed MVB path in the mining environment for the cycle a1. One can see that the LKAB path makes sharper turns than the MVB path. The LKAB path is not optimized to have a low curvature variation. (b) Cycle a1: LKAB (slashed) and MVB (solid). This subfigure shows a comparison of velocity over curve length between the LKAB path and the MVB path. It is seen that the vehicle can hold a higher speed along the MVB path compared with the speed that it can hold along the LKAB path.

TABLE II
COMPARISONS FOR CYCLES A1, A2, A3, A5, A6, C1, C2, AND C3

Cycle		t	S_{cost}	$K_{\max}$	$\dot{K}_{\max}$	s
a1	LKAB	90.8	0.01358	0.125	0.02171	183.2
	MVB	56.63	0.007523	0.1214	0.01876	184.7
	Diff (%)	**37.63**	**44.62**	**2.914**	**13.58**	**-0.8301**
a2	LKAB	84.95	0.01369	0.125	0.02171	155.9
	MVB	52.89	0.007727	0.1214	0.01876	157.3
	Diff (%)	**37.74**	**43.58**	**2.914**	**13.58**	**-0.8684**
a3	LKAB	76.95	0.01374	0.125	0.02171	130
	MVB	58.11	0.01033	0.1214	0.01885	131.6
	Diff (%)	**24.48**	**24.82**	**2.912**	**13.16**	**-1.245**
a5	LKAB	75.7	0.01373	0.131	0.02171	129.6
	MVB	54.08	0.00968	0.1214	0.01876	130.3
	Diff (%)	**28.56**	**29.49**	**7.365**	**13.58**	**-0.5315**
a6	LKAB	82.52	0.01178	0.12	0.02171	151.8
	MVB	50.11	0.007129	0.1214	0.01876	152.1
	Diff (%)	**39.28**	**39.48**	**-1.136**	**13.58**	**-0.2491**
c1	LKAB	60.41	0.01077	0.1278	0.02194	112.1
	MVB	44.06	0.005326	0.1142	0.01787	112.8
	Diff (%)	**27.08**	**50.55**	**10.6**	**18.54**	**-0.6826**
c2	LKAB	40.3	0.004429	0.1278	0.02194	79.7
	MVB	27.2	0.001884	0.1142	0.01787	80.75
	Diff (%)	**32.51**	**57.45**	**10.6**	**18.54**	**-1.32**
c3	LKAB	42.58	0.006361	0.1278	0.02194	63.56
	MVB	29.9	0.004048	0.1142	0.02188	63.42
	Diff (%)	**29.78**	**36.36**	**10.6**	**0.2729**	**0.2281**
Mean	**Diff (%)**	**32.13**	**40.79**	**5.847**	**13.10**	**-0.6873**

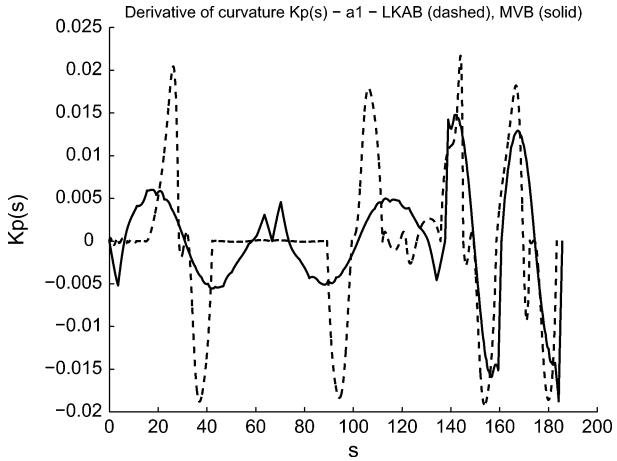

Fig. 8. Cycle a1: LKAB (dashed) and MVB (solid). The derivative of curvature is plotted both for the computed MVB path and the LKAB path. It is seen that the magnitude of the derivative of curvature is kept at an overall lower level along the MVB path than along the LKAB path.

V. CONCLUSIONS AND FUTURE WORK

Using application data from the Swedish mining company LKAB, we show that quartic uniform minimum curvature variation B-splines are suitable paths for automated four-wheel Load-Haulage-Dump vehicles in the mine. Studying eight real-world cases we show that smooth B-spline curves yield paths that are faster to drive along than paths used by LKAB today. Our simulations show that, with an average of 32.13%, the new paths are faster to travel along than the paths currently in use. Preliminary results from an internal project at LKAB show an overall 5–10% increase in ore transport production speed. Then, not only transportation is accounted for, but also moments such as loading, dumping, and maintainance. Altogether, this shows that a minimum curvature variation B-spline is suitable for high speed traversal.

Future work includes comparisons with other automatic path-planning methods. Studies of how to automatically handle the problems introduced when more than one room axis is needed. Adaptive knot placement for improving the properties of the B-spline function is of interest. An investigation of the tradeoff between higher speed and increased wear of the vehicle can be made. Investigations of the properties of the safety margin, the modeling of the vehicle, and how these affects the quality of the resulting path should be made. With the simplified vehicle model we are able to use the envelope to impose linear constraints. Using a more exact vehicle model instead of a simplified model is an interesting issue in the future. This would most probably lead to a new optimization problem setting where a more complex polygonal object collision detection method is required [34].

It is clear that our paths can be applied in other contexts than mining. It would be interesting to investigate if minimum curvature variation B-splines are efficient for use in higher dimensions and in other applications such as underwater and air space environments.

REFERENCES

[1] J.-C. Latombe, *Robot Motion Planning*. Norwell, MA: Kluwer, 1991.
[2] J. Schwartz and M. Sharir, "Algorithmic motion planning in robotics," in *Algorithms and Complexity*, J. van Leeuwen, Ed. New York: Elsevier, 1990, pp. 391–430.
[3] , K. Goldberg, D. Halperin, J.-C. Latombe, and R. Wilson, Eds., *Algorithmic Foundations of Robotics*. Wellesley, MA: A. K. Peters, 1995.
[4] Y. Hwang and N. Ahuja, "Gross motion planning—A survey," *ACM Comput. Surv.*, vol. 24, no. 3, pp. 219–291, Sep. 1992.
[5] T. Fraichard and A. Scheurer, "From reeds and shepp's to continuous curvature paths," *IEEE Trans. Robot. Automat.*, vol. 20, no. 12, pp. 1025–1035, Dec. 2004.
[6] P. Gallina and A. Gasparetto, "A technique to analytically formulate and to solve the 2-dimensional constrained trajectory planning problem for a mobile robot," *J. Intell. Robots Syst.*, vol. 27, no. 3, pp. 237–262, 2000.

[7] S. Fleury, P. Soueres, J.-P. Laumond, and R. Chatila, "Primitives for smoothing mobile robot trajectories," in *IEEE Int. Conf. Robotics Automation (ICRA)*, Las Vegas, NV, May 1993, vol. 1, pp. 832–839.
[8] A. Piazzi and A. Visioli, "Global minimum-jerk trajectory planning of robot manipulators," *IEEE Trans. Ind. Electron.*, vol. 47, no. 1, pp. 140–149, Feb. 2000.
[9] K. Komoriya and K. Tanie, "Trajectory design and control of a wheel-type mobile robot using B-spline curve," in *Proc. IEEE/RSJ Int. Workshop Intell. Robots Syst.*, Tsukuba, Japan, Sep. 1989, pp. 398–405.
[10] A. Piazzi, C. Bianco, M. Bertozzi, A. Fascioli, and A. Broggi, "Quintic g^2-splines for the iterative steering of vision based autonomous vehicles," *IEEE Trans. Intell. Transport. Syst.*, vol. 3, pp. 27–36, Mar. 2002.
[11] G. Song and N. Amato, "Randomized motion planning for car-like robots with c-prm*," in *Proc. IEEE/RSJ Int. Conf. Intell. Robots Syst.*, Maui, HI, Oct. 2001, pp. 37–42.
[12] A. Simon and J. Becker, "Vehicle guidance for an autonomous vehicle," in *Proc. IEEE/IEEJ/JSAI Int. Conf. Intell. Transport. Syst.*, Oct. 1999, pp. 429–434.
[13] M. Yamamoto, M. Iwamura, and A. Mohri, "Quasi-time-optimal motion planning of mobile platforms in the presence of obstacles," in *Proc. ICRA*, 1999, pp. 2958–2963.
[14] Luossavaara-Kiirunavaara Aktiebolag (LKAB) [Online]. Available: http://www.lkab.com.
[15] , J. E. Goodman and J. O'Rourke, Eds., *Handbook of Discrete and Computational Geometry*. Boca Raton, FL: CRC Press, 1997.
[16] L. E. Dubins, "On curves of minimal length with a constraint on average curvature and with prescribed initial and terminal positions and tangents," *Amer. J. Math.*, vol. 79, pp. 497–516, 1957.
[17] J.-D. Boissonnat, A. Cérézo, and J. Leblond, "A note on shortest paths in the plane subject to a constraint on the derivative of the curvature," in *Proc. INRIA, Rapport de Recherche 2160*, 1994 [Online]. Available: http://www.inria.fr/RRRT/RR-2160.html
[18] P. Jacobs and J. Canny, "Planning Smooth Paths for Mobile Robots," in *Nonholonomic Motion Planning*, Z. Li and J. F. Canny, Eds. Norwell, MA: Kluwer, 1992, pp. 271–342.
[19] M. de Berg, M. van Kreveld, M. Overmars, and O. Schwarzkopf, *Computational Geometry: Algorithms and Applications*. New York: Springer-Verlag, 1997.
[20] Y. Kanayama and B. I. Hartman, "Smooth local path planning for autonomous vehicles," in *Proc. 1989 IEEE Int. Conf. Robotics Automat.*, Scottsdale, AZ, 1989, vol. 3, pp. 1265–1270.
[21] C. de Boor, *A Practical Guide to Splines*. New York: Springer-Verlag, 1978.
[22] M. Cox, "The numerical evaluation of B-splines," *J. Inst. Math. Appl.*, vol. 10, pp. 134–149, 1972.
[23] P. Dierckx, *Curve and Surface Fitting with Splines*. New York: Clarendon Press, 1995.
[24] T. Berglund, T. Strömberg, H. Jonsson, and I. Söderkvist, "Epi-convergence of minimum curvature variation B-splines," Dept. Comp. Sci. Elect. Eng., Luleå Univ. Technol., Sweden, 2003, Tech. Rep. 2003:14, ISSN 1402-1536.
[25] G. Farin, *Curves and Surfaces for Computer Aided Geometric Design: A practical Guide*. Boston: Academic, 1988.
[26] D. Lutterkort and J. Peters, "Smooth paths in a polygonal channel," in *Proc. Conf. Computational Geometry (SCG'99)*, New York, Jun. 13–16, 1999, pp. 316–321.
[27] U. Reif, "Best bounds on the approximation of polynomials and splines by their control structure," *Comput. Aided Geometric Des.*, vol. 17, no. 6, pp. 579–589, 2000.
[28] T. Berglund, U. Erikson, H. Jonsson, K. Mrozek, and I. Söderkvist, M. Mohammadian, Ed., "Automatic generation of smooth paths bounded by polygonal chains," in *Proc. Int. Conf. CIMCA'2001*, Las Vegas, NV, Jul. 2001, pp. 528–535.
[29] T. Berglund, H. Jonsson, and I. Söderkvist, "An obstacle-avoiding minimum variation B-spline problem," presented at the Int. Conf. Geometric Modeling Graphics (GMAG03), London, U.K., Jul. 2003.
[30] P. Gill, W. Murray, and M. Wright, *Practical Optimization*. New York: Academic, 1981.
[31] T. Espelid, "Doubly adaptive quadrature routines based on Newton–Cote rules," Dept. Informatics, Univ. Bergen, 2002, Tech. Rep. 229.
[32] S. Tamrock, *Toro 2500 Underground Load and Haul Machine (LH625E), Retrieved* Nov. 6, 2008 [Online]. Available: http://www.miningandconstruction.sandvik.com/
[33] H. Imai and M. Iri, "Polygonal approximations of a curve—formulations and algorithms," in *Computational Morphology*, G. T. Toussaint, Ed. Amsterdam, The Netherlands: North-Holland, 1988, pp. 71–86.
[34] C. Ong and E. Gilbert, "Robot path planning with penetration growth distance," *J. Robot. Syst.*, vol. 15, no. 2, pp. 57–74, 1998.

Physical Modeling of a Bag Knot in a Robot Learning System

Uri Kartoun, *Member, IEEE*, Amir Shapiro, *Member, IEEE*, Helman Stern, *Member, IEEE*, and Yael Edan, *Member, IEEE*

***Abstract*—This paper presents a physical model developed to find the directions of forces and moments required to open a plastic bag—which forces will contribute toward opening the knot and which forces will lock it further. The analysis is part of the implementation of a $Q(\lambda)$-learning algorithm on a robot system. The learning task is to let a fixed-arm robot observe the position of a plastic bag located on a platform, grasp it, and learn how to shake out its contents in minimum time. The physical model proves that the learned optimal bag shaking policy is consistent with the physical model and shows that there were no subjective influences. Experimental results show that the learned policy actually converged to the best policy.**

***Note to Practitioners*—This paper was motivated by the problem of developing a physical model capable of finding the directions of force and moments required to open a knotted plastic bag—which forces will contribute toward opening the knot and which forces will lock it further. The analysis was part of the implementation of a reinforcement-learning algorithm for a fixed-arm robot system called "RoboShake." The learning task was to observe the position of a bag contains suspicious items (such as biological or chemical items), grasp it, and learn the optimal sequence of motions to shake out its contents in minimum time. An extremely interesting finding was the fact that the robot's optimal policy always converged to a one that was consistent with Newton's three laws of motion. The system learned the optimal policies by interaction with the environment without using these laws as part of the system design/implementation. From a philosophical aspect, the experimental robotic platform found solutions that were consistent with Newton's laws of motion, i.e., the system was capable of explaining Newton's laws of motion without being "aware" of them, and in a way, and to "discover" the existence of the second and the third laws. Experimental systems of this kind, especially if designed with a capability to carry out new experiments independently, may help to explain, discover, or predict laws/rules (not necessarily of machines/robots) that are not known to us yet.**

***Index Terms*—Intelligent robots, reinforcement learning, robot kinematics, robot learning.**

I. Introduction

To expand the use of robots in everyday tasks they must be able to perform in unpredictable and continuously changing environments. Since it is impossible to model all environments and task conditions in a rigorous enough manner, robots must learn independently how to respond to the world and how the world responds to actions they take.

One approach to robot learning is reinforcement learning (RL) (e.g., [1]–[9]). In RL, the robot receives positive/negative rewards from the environment indicating how well it performs the required task. The

Manuscript received April 02, 2008; revised September 13, 2008. First published May 08, 2009; current version published January 08, 2010. This paper was recommended for publication by Associate Editor Y.-B. Jia and Editor V. Kumar upon evaluation of the reviewers' comments. This work was supported in part by the Paul Ivanier Center for Robotics Research and Production Management, in part by the Rabbi W. Gunther Plaut Chair in Manufacturing Engineering, and in part by the Pearlstone Center for Aeronautical Engineering, Ben-Gurion University of the Negev.

U. Kartoun, H. Stern, and Y. Edan are with the Department of Industrial Engineering and Management, Ben-Gurion University of the Negev, Beer-Sheva 84105, Israel (e-mail: kartoun@bgu.ac.il; helman@bgu.ac.il; yael@bgu.ac.il).

A. Shapiro is with the Department of Mechanical Engineering, Ben-Gurion University of the Negev, Beer-Sheva 84105, Israel (e-mail: ashapiro@bgu.ac.il).

Color versions of one or more of the figures in this paper are available online at http://ieeexplore.ieee.org.

Digital Object Identifier 10.1109/TASE.2009.2013133